Geol. Mag. **155** (3), 2018, pp. 630–640. © Cambridge University Press 2016
doi:10.1017/S001675681600090X

Kinematic evolution of a fold-and-thrust belt developed during basin inversion: the Mesozoic Maestrat basin, E Iberian Chain

MARINA NEBOT* & JOAN GUIMERÀ

Geomodels Research Institute, Departament de Dinàmica de la Terra i de l'Oceà, Facultat de Geologia, Universitat de Barcelona (UB), Martí i Franquès s/n, 08028 Barcelona, Spain

(*Received* 25 April 2016; *accepted* 29 August 2016; *first published online* 4 October 2016)

Abstract – The Maestrat basin was one of the most subsident basins of the Mesozoic Iberian Rift system, developed by a normal fault system which divided it into sub-basins. Its Cenozoic inversion generated the N-verging Portalrubio–Vandellòs fold-and-thrust belt in its northern margin, detached in the Triassic evaporites. In the hinterland, a 40 km wide uplifted area, in the N–S direction, developed, bounded to the N by the E–W-trending, N-verging Calders monocline. This monocline is interpreted as a fault-bend fold over the ramp to flat transition of the E–W-trending, N-verging Maestrat Basement Thrust, and also indicates the transition from a thick-skinned (S) to a thin-skinned (N) style of deformation. This paper presents a kinematic evolutionary model for the northern margin of the basin and a reconstruction of the Maestrat Basement Thrust geometry, generated by the inversion of the Mesozoic normal fault system. It contains a low-dip ramp (9°) extended southwards more than 40 km, attaining a depth of 7.5 km. As this thrust reached the Mesozoic cover to the foreland, it propagated across the Middle Muschelkalk evaporitic detachment, generating a nearly horizontal thrust which transported northwards the supra-salt cover, and the normal fault segments within it, for *c.* 11–13 km. The displacement of the basement in the hanging-wall of the low-dip basement ramp generated the 40 km wide uplifted area, while the superficial shortening was accumulated in the northern margin of the basin – which contains the thinnest Mesozoic cover – developing the Portalrubio–Vandellòs fold-and-thrust belt.

Keywords: basin inversion, low-dip ramp, tectonic relief, salient, fold-and-thrust belt.

1. Introduction

The Linking Zone resulted from the Cenozoic inversion of the Mesozoic Maestrat basin, located between the NW–SE-trending Iberian Chain and the NE–SW-trending Catalan Coastal Chain (Guimerà, 1984, 1988; Fig. 1). Its northern part contains the Portalrubio–Vandellòs fold-and-thrust belt, broadly E–W-trending and N-verging, while a wide tectonically elevated area developed in its southern part (Guimerà, 1988; Guimerà *et al.* 2010). Nebot & Guimerà (2016) recognized a new structure separating these two areas, the decakilometric-scale Calders monocline (Figs 2, 3), interpreting it as a fault-bend fold over ramp to flat geometries of a deep-seated thrust (the Maestrat Basement Thrust; Nebot & Guimerà, 2016). The aim of this paper is to provide new data to support the interpretations of Nebot & Guimerà (2016) and to establish the kinematic evolution of the fold-and-thrust belt. More specifically, the objectives of this paper are (i) to estimate the shortening of the fold-and-thrust belt, located N of the Maestrat Basement Thrust ramp, and (ii) to characterize the Mesozoic extensional structure whose Cenozoic contractional inversion developed the belt.

With this purpose, two new cross-sections have been constructed, containing the deduced transport orientation. Determining the shortening in this area is complex as, on the one hand, main structures show varying orientations and, on the other hand, late to post-tectonic Cenozoic outcrops cover some areas which otherwise would be the most suitable for the regional cross-section construction. Moreover, the thickness of the Mesozoic cover is difficult to establish, as its base hardly ever crops out and no subsurface data are available. Nevertheless, new Lower Cretaceous stratigraphic sections were also obtained from new field data which, combined with previous stratigraphic data, permitted the characterization of the syn-sedimentary extensional structure during this period.

After these data, a palinspastic restoration of the main structures during the Early Cretaceous is proposed, as well as a reconstruction of the geometry of the Maestrat Basement Thrust, more accurate than that proposed by Nebot & Guimerà (2016). Finally, this paper presents a kinematic evolutionary model for the N margin of the inverted Maestrat basin, which constitutes a good example of a fold-and-thrust belt developed during basin inversion, presenting in its foreland a thin-skinned fold-and-thrust belt conditioned by an evaporitic detachment level, while in its thick-skinned hinterland generated the uplift of a wide area.

2. Geological setting

The Iberian Chain developed during the Cenozoic Alpine orogeny, as a result of the contractional

*Authors for correspondence: marinanebotmiralles@gmail.com

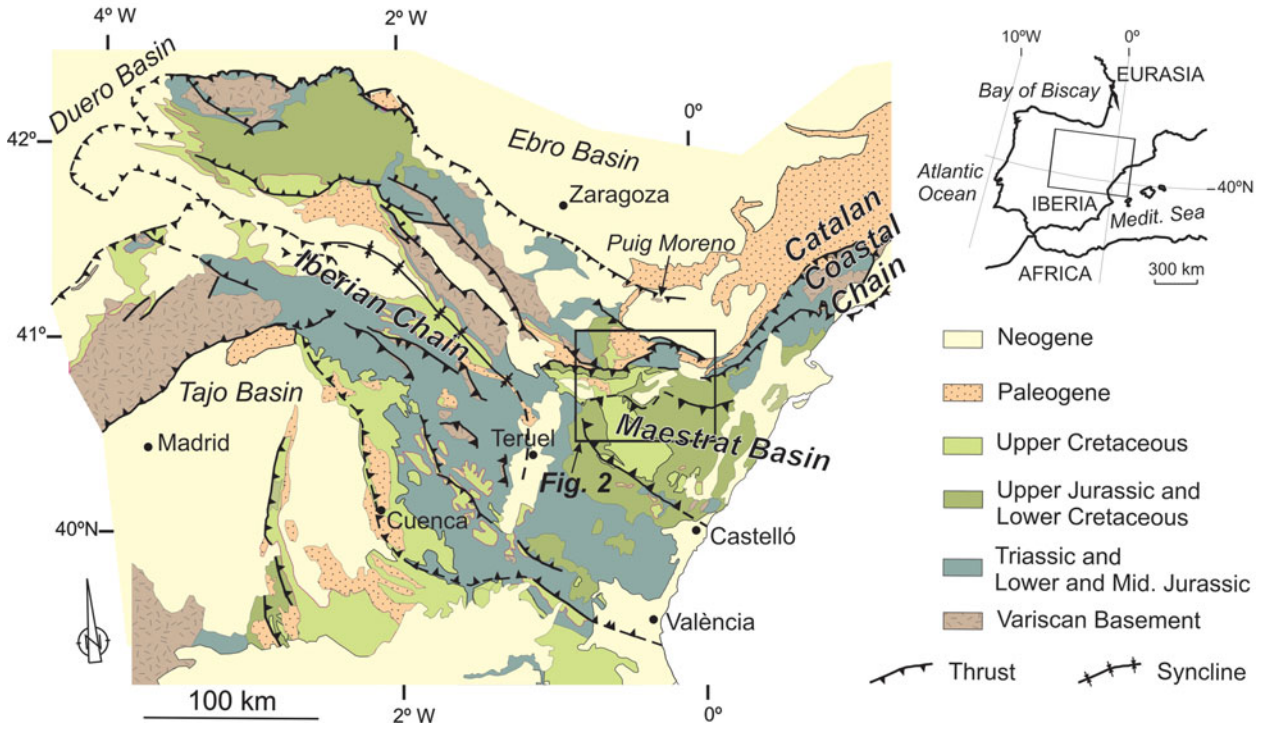

Figure 1. (Colour online) Simplified geological map of the Iberian Chain, and its location in the eastern Iberian Peninsula. Location of the area studied (Fig. 2) is also shown. Modified from Nebot & Guimerà (2016) after Guimerà (2004).

inversion of the Iberian Rift System (Álvaro, Capote & Vegas, 1979; Salas *et al.* 2001; Guimerà, Mas & Alonso, 2004), which was active during the Mesozoic, and experienced two main rifting events, during the Late Permian – Late Triassic and during the Late Oxfordian – Late Albian (Fig. 4; Salas *et al.* 2001), followed by events of lower rifting activity (Early and Middle Jurassic, and Late Albian to Maastrichtian).

The Maestrat basin was one of the most subsident basins within the Iberian Rift System, developed during the Jurassic to Early Cretaceous rifting event. Its sedimentary filling was dominated by shallow marine to lacustrine carbonates, with intercalations of continental siliciclastic sediments, and a few intercalations of pelagic sediments (R. Salas, unpub. Ph.D. thesis, Univ. Barcelona, 1987). Some evaporitic layers are recognized in the Triassic: the Keuper and the Middle Muschelkalk. The latter was the regional detachment during the Cenozoic contraction, differentiating two structural packages (Fig. 3): the supra-salt cover (units above the Middle Muschelkalk) and the sub-salt or acoustic basement (units below the Middle Muschelkalk) (Nebot & Guimerà, 2016).

The Cenozoic inversion of the northern margin of the Maestrat basin generated the Portalrubio–Vandellòs fold-and-thrust belt (Guimerà, 1988), in the northern part of the Linking Zone (Fig. 3). In the study area, this fold-and-thrust belt displays a salient (in the sense of Marshak, 2004), as traces of thrusts and folds take curved shapes convex to the N, in the sense of transport (Fig. 3). Therefore the adjacent areas of Ejulve–Aliaga and Herbers (Fig. 3) could be associated with recesses containing superposition of structures with different orientations (Simón, 1980; Guimerà, 1988).

South of this fold-and-thrust belt, the E–W-trending Calders monocline bounds to the north the tectonically elevated area (Nebot & Guimerà, 2016; Figs 2, 3). This monocline has been interpreted as a fault-bend fold that is the surface expression of the ramp–flat geometry of the Maestrat Basement Thrust in the study area, resulting from the Cenozoic inversion of the Mesozoic extensional fault system of the Maestrat basin across the basement (Nebot & Guimerà, 2016). A vertical tectonic step of 800–1200 m can be measured above the Calders monocline (Fig. 3; González, Guimerà & Luzón, 1998; Nebot & Guimerà, 2016) whose tilted limb dips *c.* 5° N and is 13 km wide in its central part, narrowing laterally (Fig. 2).

3. Methodology

About 1200 new strike-and-dip data were obtained both in the field and from 3D geological contacts drawn on ortho-images and 3D topographic contour lines in a georeferenced environment (Microstation®), using in-house macros developed by O. Fernández (unpub. Ph.D. thesis, Univ. Barcelona, 2004). Based on these new strike-and-dip data, new mapping after field work and ortho-image interpretation, and also the previous geological maps (Canérot & Leyva, 1972; Canérot & Pignatelli, 1972, 1977; Esnaola & Canérot, 1972; Martín, Leyva & Canérot, 1972; Navarro-Vázquez *et al.* 1972; Marín *et al.* 1974; Almela *et al.* 1975; Marín & Duval, 1976; Canérot, Crespo-Zamorano & Navarro-Vázquez,

https://doi.org/10.1017/S001675681600090X Published online by Cambridge University Press

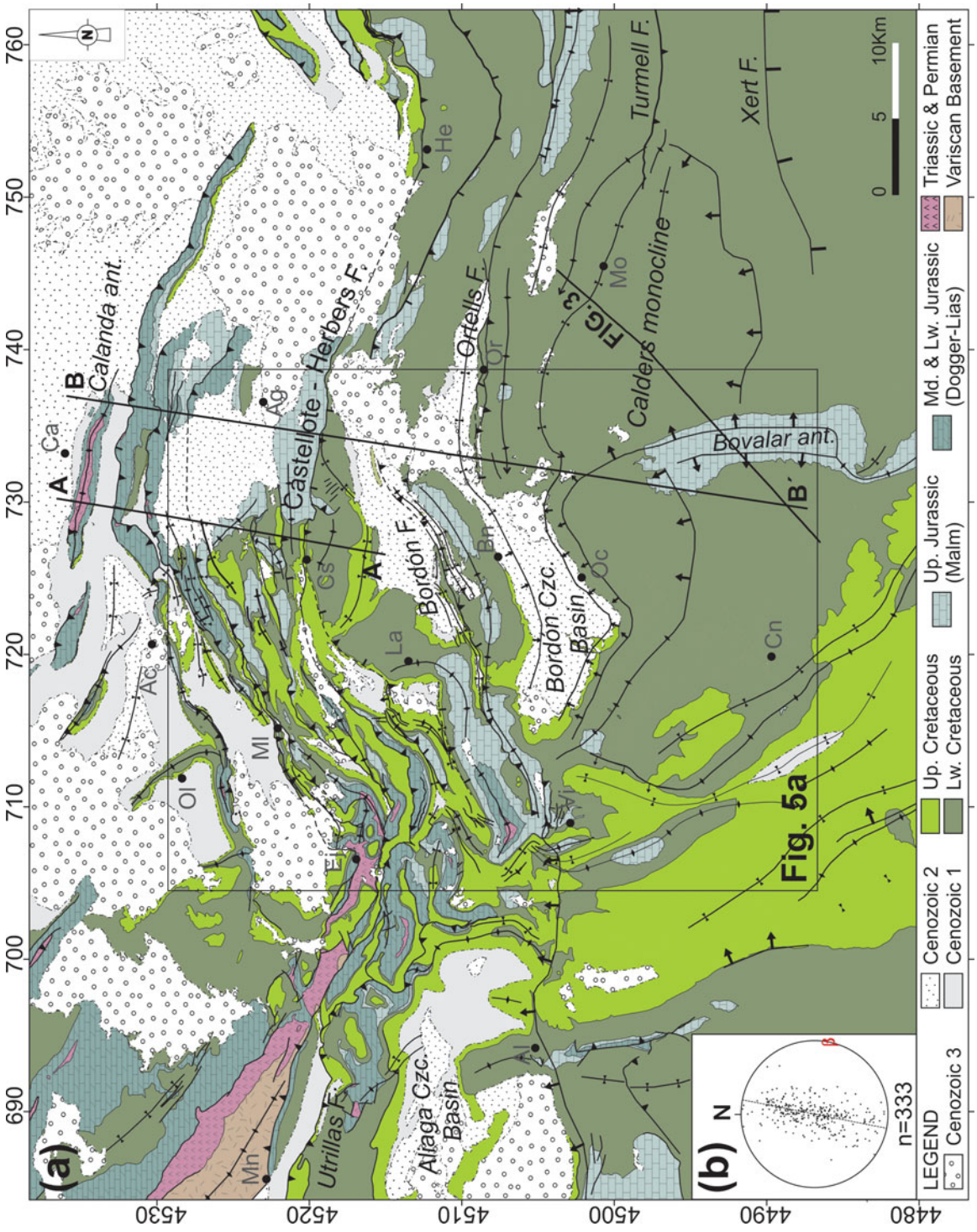

Figure 2. (Colour online) (a) Geological map of the Linking Zone between the Iberian Chain and the Catalan Coastal Chain. The Portalrubio–Vandellòs fold-and-thrust belt is located in its northern part. Cenozoic 1, 2 and 3 are the pre-orogenic, syn-orogenic and late to post-orogenic units, respectively (based on González, 1989). See location in Figure 1. Villages: Ac – Alcorisa; Ag – Aiguaviva; Al – Aliaga; Bn – Bordón; Ca – Calanda; Cn – Cantavieja; Cs – Castellote; Ej – Ejulve; He – Herbers; La – Ladruñán; Mo – Morella; Mn – Montalbán; Ml – Molinos; Oc – Olocau del Rei; Ol – Oliete; Or – Ortells, Vi – Villarluengo. Abbreviations: Czc.-Cenozoic; F.-fault; ant.- anticline. The location of the map in Figure 5a, the seismic profile in Figure 3, and the cross-sections in Figure 6 are shown. UTM projection (Zone 30 N, coordinates in km), ED50 datum. (b) Lower hemisphere spherical equal-area projection of bedding, corresponding to the cross-section traces. n = number of data, dashed line = cyclograph of the best-fit plane of the strike-and-dip data, β = pole of the cyclograph, used as projection vector of data to the cross-section plane.

https://doi.org/10.1017/S001675681600090X Published online by Cambridge University Press

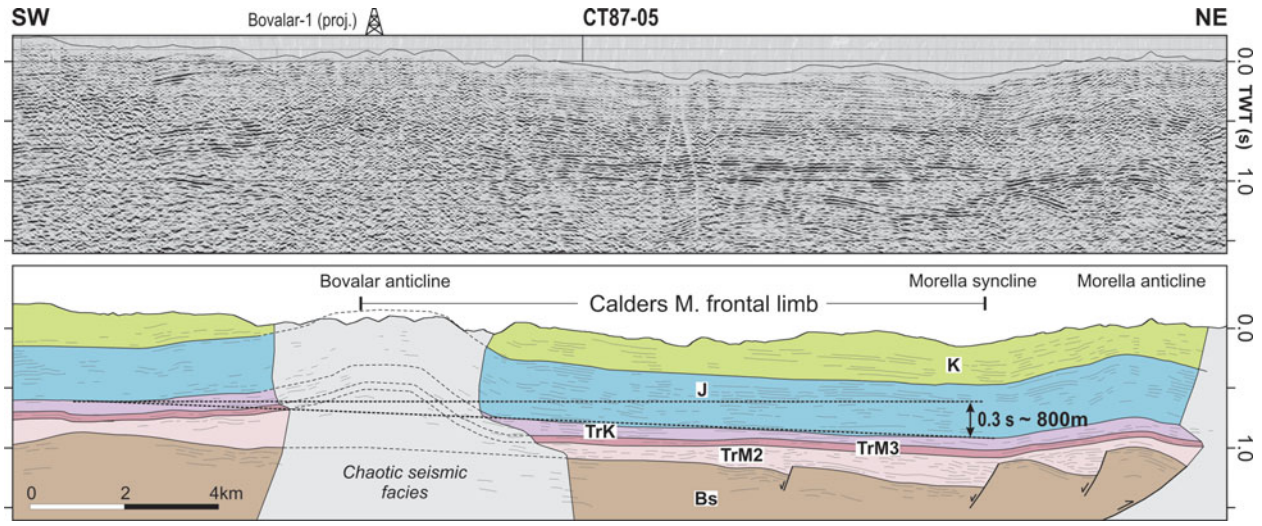

Figure 3. (Colour online) Seismic profile CT87-05 and its interpretation. It shows a wide area of gentle dip towards the N, the frontal tilted limb of the Calders monocline (Nebot & Guimerà, 2016). Abbreviations: K– Cretaceous; J – Jurassic; TrK – Keuper; TrM3 – Upper Muschelkalk; TrM2 – Middle Muschelkalk; Bs – acoustic basement. See Figure 2 for location. Modified from Nebot & Guimerà (2016).

1977; Gautier, 1978, 1979; González, 1989), two cross-sections were constructed and restored, and a complete geological map of the study area was made.

Cross-section constructions – based on the Kink method – and their restoration using the flexural-slip unfolding algorithm were performed with the Move® software. An idealized cross-section of the entire N margin of the basin was also elaborated by combining different cross-section segments, which allowed us to reconstruct, with the Move® software, the geometry of the basement fault that fits the generation of the elevated area during the Cenozoic inversion. The seismic profiles and the exploration wells available S of the study area (Lanaja, 1987; Nebot & Guimerà, 2016) were also considered, in order to estimate the structure and the thicknesses of stratigraphic units which do not crop out in the study area (Fig. 4).

4. Mesozoic extensional structure

Thicknesses of the syn-rift Lower Cretaceous filling of the Maestrat basin (Fig. 5) were established from field data, exploration wells and after R. Salas (unpub. Ph.D. thesis, Univ. Barcelona, 1987). Significant thickness variations were found in the Barremian units, while the Aptian units have a more constant thickness (Fig. 5). After these variations, the Maestrat basin is divided into two zones: (1) the northern external zone (Salas & Guimerà, 1996), containing a very thin or no Lower Cretaceous rocks, and (2) the Salzedella sub-basin (Salas & Guimerà, 1996; Nebot & Guimerà, 2016), which contains the Ladruñán zone with intermediate characteristics (Fig. 5).

The Salzedella sub-basin is located in the hanging-wall of the Castellote–Herbers and the Garrocha normal faults, while other Mesozoic faults are found within it (Fig. 5a). The Ladruñán zone is located at the NW end of the Salzedella sub-basin, separated by the Bordón and the Villarluengo normal faults, and merges towards the E with the Salzedella sub-basin (Fig. 5a). In the northern external zone, the Barremian and Aptian units are concentrated in the outcrops located N of Castellote (Figs 5a, 6A–A′) and N of Aiguaviva (Figs 5a, 6B–B′). The distribution of the Lower Cretaceous rocks and the varying orientation of structures suggest a segmented system of normal faults connected by relay ramps bounding the different zones (Fig. 5a).

The Jurassic broadly becomes thinner towards the N (Nebot & Guimerà, 2016), with major thickness variations in the syn-rift Malm and in the Lower Lias units (Figs 4, 5a). Regarding the Triassic, the lower Triassic units are only known by sub-surface data in the S part of the study area. To construct the cross-sections in Figure 6, an average value of 500–400 m was considered for the Middle Muschelkalk, estimated after the analysis of the isopach map obtained by Nebot & Guimerà (2016). Towards the N the Middle Muschelkalk becomes thinner, as wells in the Ebro basin reveal an average thickness of 200 m (Lanaja, 1987).

5. Cenozoic contractional structure

5.a. Structural style variations

Three main structural domains were differentiated in the study area (Fig. 7), based on the new field work here presented and also the previous work of Guimerà (1988) and Nebot & Guimerà (2016).

5.a.1. Southern slightly deformed area

This area contains the 40 km wide – in the N–S direction – tectonically elevated area (Fig. 7), developed in the hanging-wall of the Maestrat Basement Thrust, and the Calders monocline, which bounds it to the N,

https://doi.org/10.1017/S001675681600090X Published online by Cambridge University Press

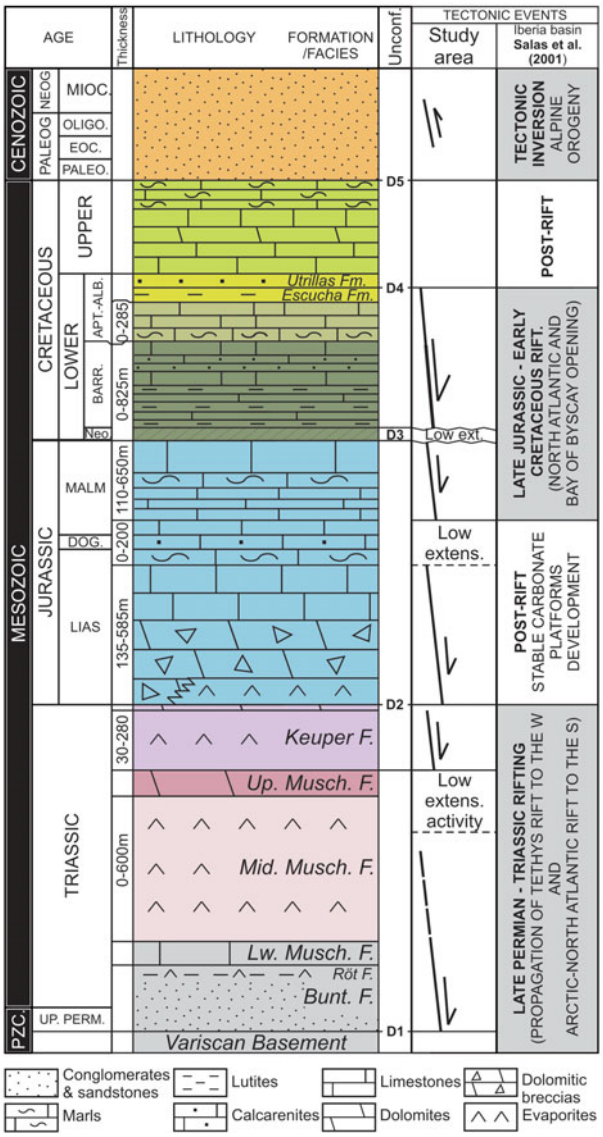

Figure 4. (Colour online) Generalized stratigraphic sequence of the Eastern Salzedella sub-basin. Modified from Nebot & Guimerà (2016), after R. Salas (unpub. Ph.D. thesis, Univ. Barcelona, 1987), Salas *et al.* (2001), Aurell *et al.* (1992) for the Lias, and Bover-Arnal *et al.* (2015) for the Barremian–Aptian boundary.

therefore it is located over the transition from ramp to flat of the Maestrat Basement Thrust (Nebot & Guimerà, 2016). Structures at the surface have kilometric wavelengths and are rooted mostly in the acoustic basement, although detachment folds developed, rooted in the Middle Muschelkalk evaporites (Guimerà, 1988; Nebot & Guimerà, 2016).

5.a.2. Intermediate area

This area is characterized by folds of kilometric wavelengths detached in the Middle Muschelkalk, although some fragments of the acoustic basement are also incorporated in the thrust sheets. It is bounded to the N by the Castellote–Herbers Fault and to the S by the Calders monocline synformal frontal hinge (Fig. 7).

5.a.3. Northern frontal fold-and-thrust belt (N FAT belt)

The northern part of the study area is characterized by tight structures, with wavelengths of hundreds of metres to a few kilometres. They are detached in the Triassic units (Middle Muschelkalk and locally in the Keuper), and in some cases also incorporate fragments of the acoustic basement in the hanging-wall of the thrust sheets (Figs 6, 7). This area coincides with the northern external zone of the Maestrat basin, containing the thinnest supra-salt cover (Fig. 7). The Calanda anticline, the northernmost structure of this fold-and-thrust belt, is detached in the Middle Muschelkalk (Fig. 6) as Upper Muschelkalk rocks crop out in its core (Anadón & Albert, 1973).

In the most frontal part of the fold-and-thrust belt, the major thrust-sheet displacement is transferred towards the foreland from the W, where it is concentrated in the Molinos thrust sheet (Fig. 2), to the E, accumulated mostly in the Calanda thrust sheet (Fig. 6).

SW of the Calanda anticline, structures change their trend from ESE–WNW and E–W to NE–SW, as they display the salient geometry, convex to the N, previously described. In this area, the *N FAT belt* structures and the NW–SE-trending structures of the Iberian Chain converge, producing fold interferences (Simón, 1980, 2004; Guimerà, 1988) and a NE–SW-trending back-thrust in the convergence area (Fig. 2).

5.b. Inversion structures

Some normal faults were partially inverted as thrusts, which inherited their orientations, folding the Upper Cretaceous post-rift in the Garrocha fault or the Ortells fault in its eastern part (Figs 2, 6B–B′). In other cases, the Upper Cretaceous post-rift was thrusted by the inverted fault, their slips being of only a few metres, and the extensional slip being not recovered, as in the Bordón fault (Fig. 2). These two cases are observed in the Castellote fault, which changes the amount of inversion along-strike, being minimum in its western NE–SW-trending segment, where the Upper Cretaceous post-rift is only folded (Fig. 2), and increasing to the E, where the Upper Cretaceous is thrusted in its E–W-trending segment (Fig. 6). Newly formed thrusts also appeared, most of them in the N external zone.

5.c. Transport direction and estimated shortening

Most structures in the Linking Zone are ESE–WNW-trending, parallel to the Calders monocline trace (Fig. 7b), such as the Calanda anticline and the two thrust sheets south of it, the Castellote fault in its northernmost segment, the Ortells fault, or the overall strike of the Utrillas fault (Fig. 2). Therefore, the transport direction is assumed to be parallel to the vector normal to these ESE–WNW-trending structures, and the sense of transport to the foreland, hence to the NNE, which coincides with the one proposed by Guimerà & Álvaro (1990) for the Iberian Chain.

https://doi.org/10.1017/S001675681600090X Published online by Cambridge University Press

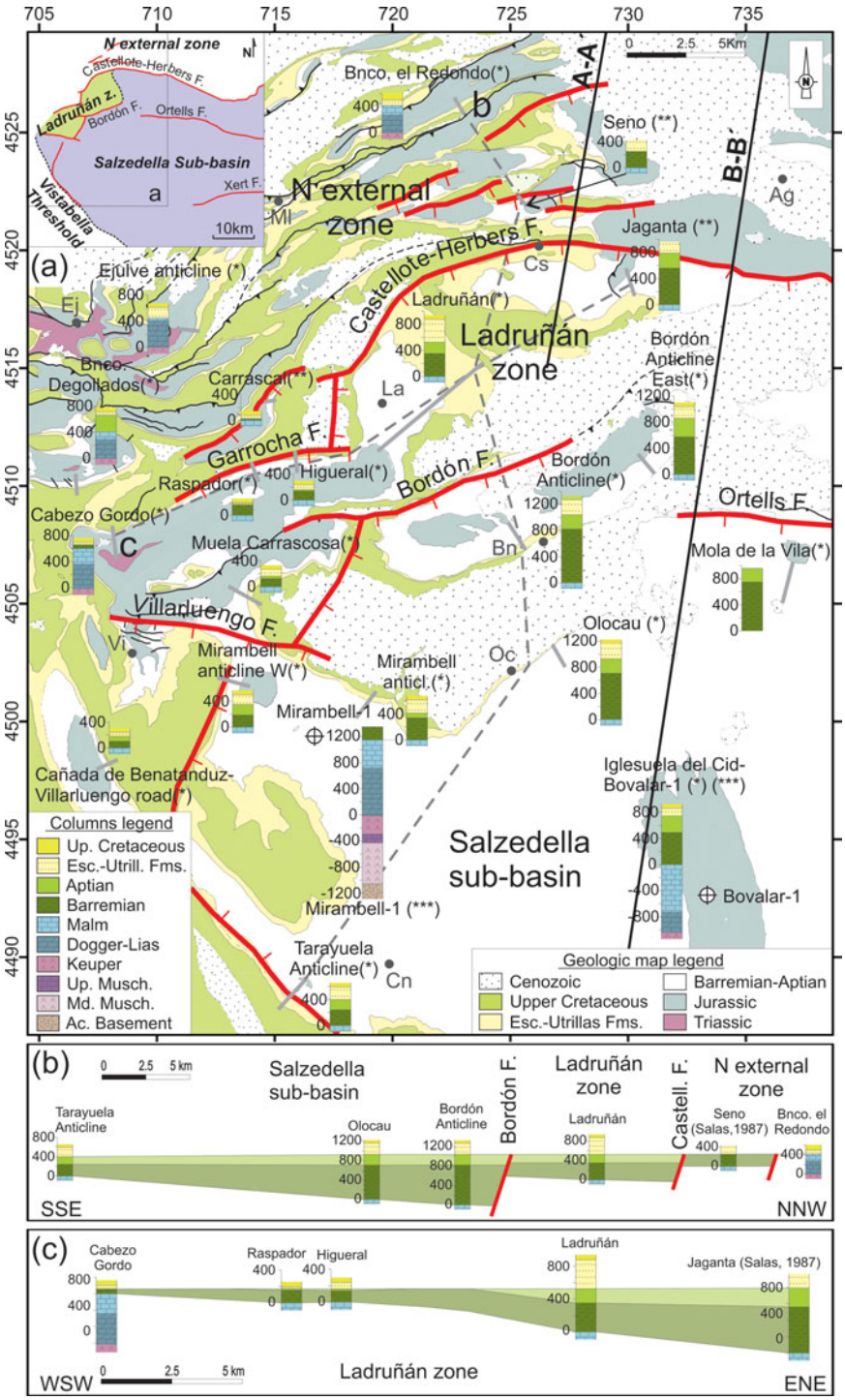

Figure 5. (Colour online) (a) Stratigraphic sections of the studied area, and the main tectonostratigraphic domains recognized and the structures bounding them. The normal faults interpreted for the Barremian and Aptian period are shown. The stratigraphic sections were obtained from new field data (*) and were combined with sections obtained by R. Salas (unpub. Ph.D. thesis, Univ. Barcelona, 1987) (**), and with sub-surface data (***) (exploration wells after Lanaja, 1987, and seismic data converted to depth by Nebot & Guimerà, 2016). (b, c) Simplified correlation of the Barremian and Aptian units in some stratigraphic sections in directions roughly perpendicular (b) and parallel (c) to the geological structures. Different tectonostratigraphic domains and the structures bounding them are depicted. The datum is the base of the Escucha Fm. (top of the Aptian), as this formation developed small sub-basins different from the Barremian–Aptian ones.

Two cross-sections were constructed containing the NNE–SSW transport direction: a regional cross-section that intersects the Calders monocline near its central part (Fig. 6B–B′) and a more local one placed *c.* 7 km W of this regional cross-section (Fig. 6A–A′). The shortening estimated by restoring the regional cross-section (Fig. 6B–B′) is of *c.* 10.5 km, which can be considered a minimum value for the N margin of the Maestrat basin, as cross-sections were constructed in a conservative manner, not including the deformation

https://doi.org/10.1017/S001675681600090X Published online by Cambridge University Press

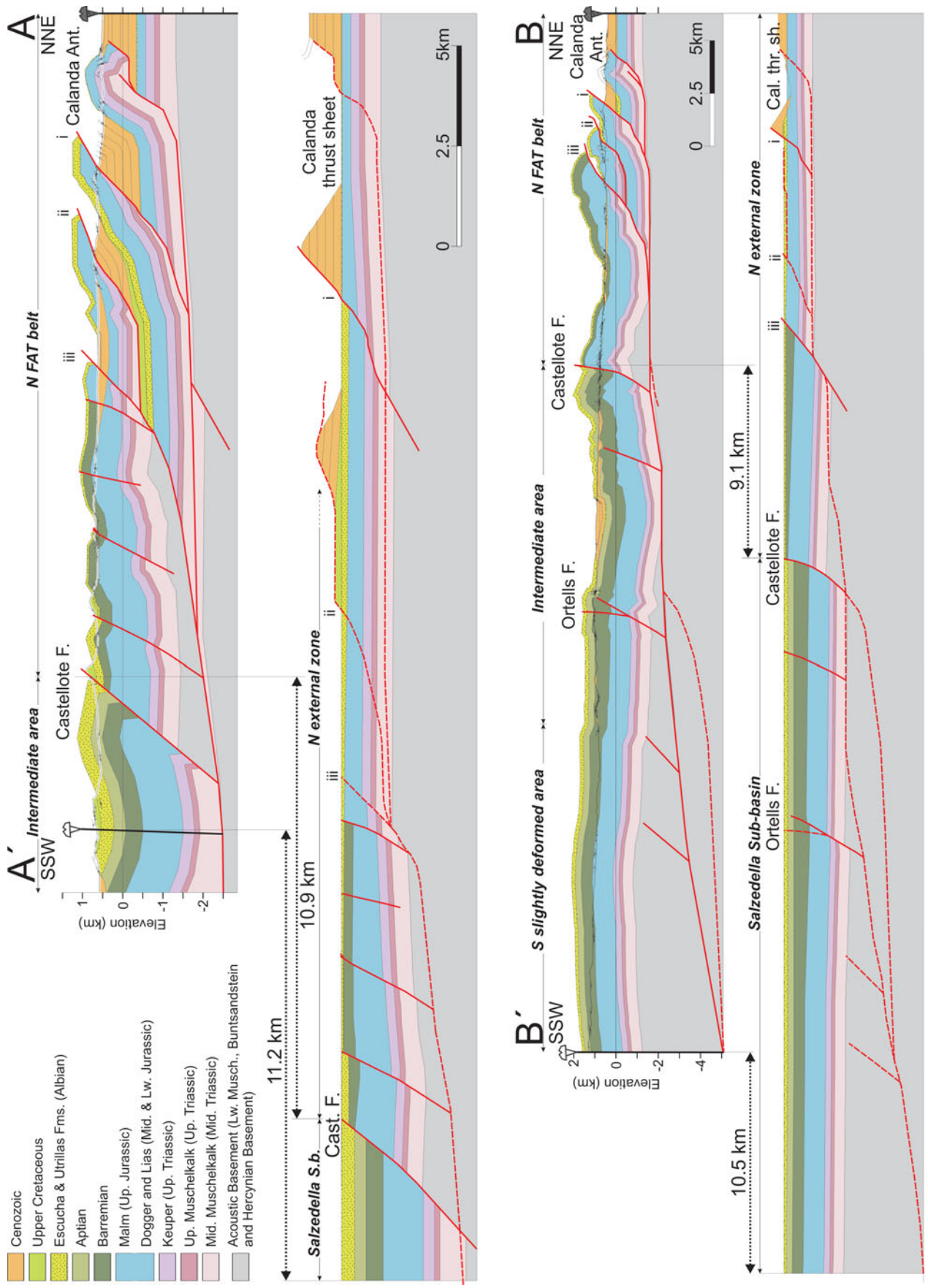

Figure 6. (Colour online) Cross-sections A–A′ and B–B′. See location in Figure 2. They contain the NNE–SSW transport direction.

https://doi.org/10.1017/S001675681600090X Published online by Cambridge University Press

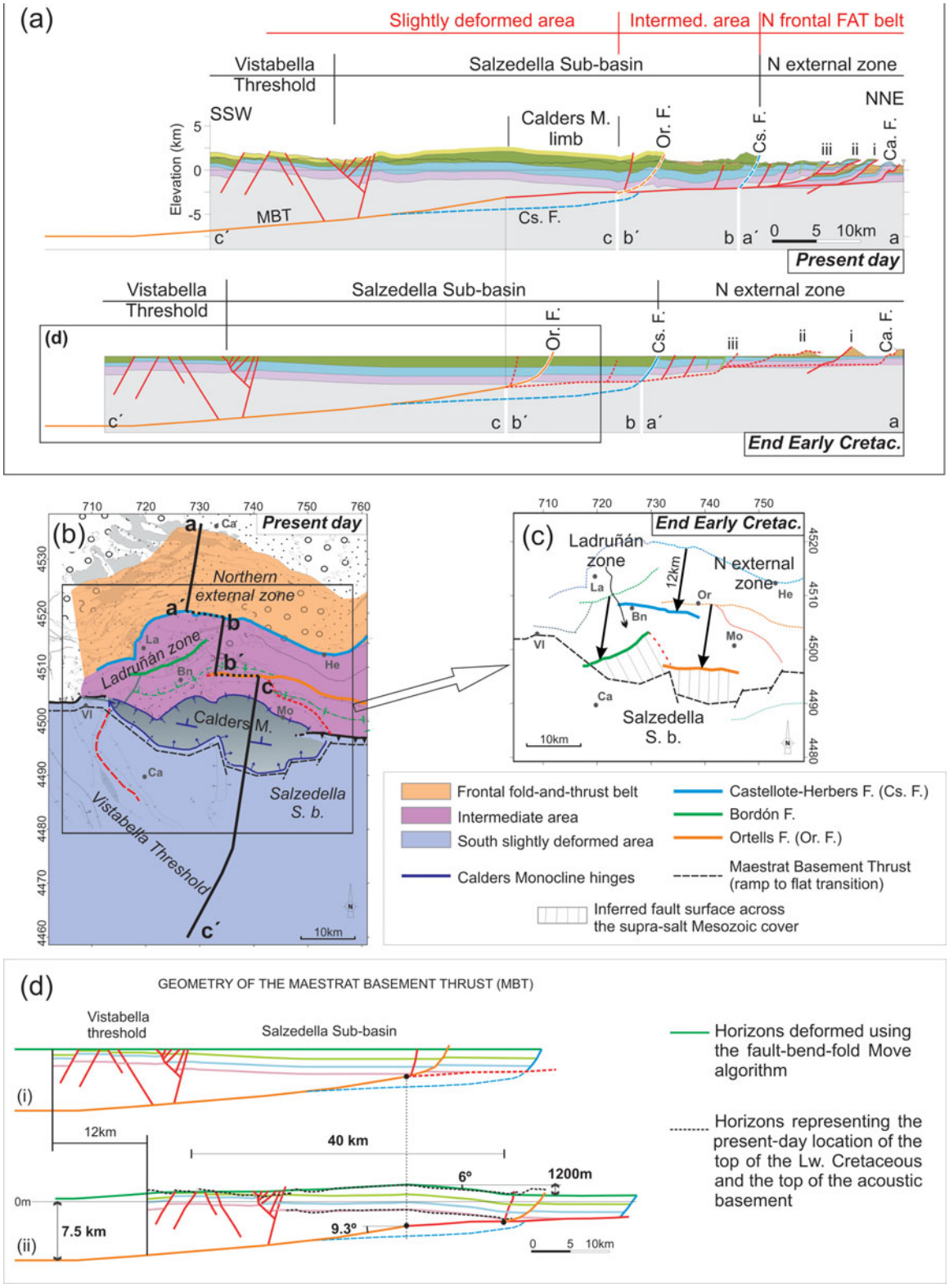

Figure 7. (Colour online) (a) Idealized section of the study area, obtained by combining cross sections A–A′, B–B′ (Fig. 6) and an unpublished cross-section from Guimerà. The interpreted evolution of the area studied is shown. (b) Simplified structural map of the Cenozoic structures developed after the Maestrat basin inversion. Modified from Nebot & Guimerà (2016). (c) Palinspastic restoration of the normal faults within the Maestrat basin at the end of the Mesozoic extension (end of the Early Cretaceous). (d. i) Idealized section of the Salzedella sub-basin at the end of the Mesozoic extension (end of the Early Cretaceous). It is based on the generalized section in (a). (d. ii) Forward modelling of section (d. i) using the fault-bend-fold deformation algorithm with Move®. The resulting horizons are compared to the corresponding horizons in the idealized section in (a) in order to test the geometry of the Maestrat Basement Thrust. The Castellote normal fault was not inverted in this model. Its upper segment across the supra-salt cover was only passively transported within the thrust system.

https://doi.org/10.1017/S001675681600090X Published online by Cambridge University Press

associated with mesostructures, and also, the structures below the wide Cenozoic outcrops intersected by this cross-section were simplified and could accumulate additional shortening. The shortening obtained for the cross-section A–A′, which intersects mainly the frontal fold-and-thrust belt, is 11.2 km. The shortening measured in the *N FAT belt* – placing the pin line in the Cenozoic rocks in the footwall of the Calanda thrust sheet, and the loose line in the Castellote fault – is of 10.9 km (40 %) in the cross-section A–A′ and of 9.1 km (35 %) in the cross-section B–B′. Assuming that shortening does not vary laterally in this ESE–WNW-trending part of the *N FAT belt*, cross-section B–B′ could accumulate *c.* 1.8 km of additional shortening in the *N FAT belt*, which was not recorded in cross-section B–B′ due to the Cenozoic rocks covering some of the Mesozoic outcrops. Consequently, it could reach a total shortening of 12.3 km (Fig. 6B–B′).

5.d. Geometry of the Maestrat Basement Thrust

To explain the wide uplifted area in the hinterland, Nebot & Guimerà (2016) proposed a very low-dip ramp for the Maestrat Basement Thrust, deduced after the geometry of the Calders monocline. The present work presents a more accurate reconstruction that takes into account the estimated shortening in the northern margin of the Maestrat basin just presented. This reconstruction was modelled with the Move® software, and was tested by displacing the restored horizons of the Salzedella sub-basin in the idealized cross-section (Fig. 7a), above the hanging wall of this fault, using the fault-bend-fold algorithm, until obtaining a geometry similar to that observed in the study area and until the upper segments of the normal faults across the supra-salt cover are placed in their present-day location. To achieve this, a displacement of 12 km was needed, giving additional support to the shortening value estimated after restoring the cross-sections.

The resulting fault (Fig. 7d) has a low-dip ramp, with an approximately listric geometry, which dips *c.* 9° in its shallowest part, flattening downwards, until reaching a depth of 7.5 km below sea level, extending southwards for more than 40 km. When the restored horizons of the Salzedella sub-basin (Fig. 7d.i) are transported above this fault for 12 km, a wide flat area is uplifted in its hanging-wall, while a fault-bend fold, similar to the Calders monocline, is generated above the transition from ramp (S) to flat (N) of the fault, whose frontal tilted limb is *c.* 12 km wide and dips *c.* 6° towards the N. A vertical step of 1200 m is obtained between horizons in the uplifted area and in the downthrown area (Fig. 7d.ii).

6. Discussion

6.a. Shortening in the Maestrat basin northern margin

Shortening in the Mesozoic supra-salt cover concentrates mostly in the frontal fold-and-thrust belt, while southwards, in the intermediate and southern areas, the thrust sheets experienced low internal deformation by folding and partial inversion of the Mesozoic normal faults. In the sub-salt basement, shortening accumulated in a more internal and lower position, where the thrust sheet involves the basement (Fig. 7a).

The shortening obtained by restoring the regional cross-section (*c.* 12 km; Fig. 7B–B′) is less than the maximum 13 km estimated after analysing the geometry of the Calders monocline (Nebot & Guimerà, 2016). This difference may result from the fact that the regional cross-section does not cross the widest part of the Calders monocline, and also that the cross-sections were constructed in a conservative manner, and could accumulate more shortening.

Although the Calders monocline geometry suggests a differential shortening, as it narrows laterally (Nebot & Guimerà, 2016), the thrust-sheet displacement does not disappear at the lateral ends of the monocline, as it is transmitted to other structures, indicating that the geometry of the Maestrat Basement Thrust changes laterally, out of the area studied.

6.b. Kinematic evolution

The Mesozoic extensional fault system was inverted in its lower segment across the acoustic basement, generating the Maestrat Basement Thrust. As this thrust reached the Mesozoic cover, rather than inverting the normal fault segments across the supra-salt cover, a nearly horizontal short-cut developed, propagating to the N within the Middle Muschelkalk evaporites, producing the deduced ramp–flat geometry (Fig. 7a).

It continued to the N, shallowing progressively as the Mesozoic cover became thinner towards the N, cutting across a fragment of the acoustic basement in the footwall of the Castellote fault (Fig. 6), and in the footwall of the main normal faults, incorporating the acoustic basement into the thrust sheets and transporting it to the N within the thin-skinned fold-and-thrust belt (Figs 6, 7). The sole thrust ends up in the Calanda thrust sheet, expressed at the surface as the Calanda anticline (Figs 6, 7a). As previously explained, wavelengths of the contractional structures decrease to the N, as a result of the thinning of the Mesozoic cover (Fig. 7a).

About 22 km N of the Calanda anticline, an isolated outcrop of Paleozoic rocks is found among the Cenozoic rocks of the Ebro foreland basin, the Puig Moreno outcrop (Fig. 1). In order to explain it, Salas *et al.* (2001) interpreted a more frontal basement thrust which towards the S branches to the Maestrat Basement Thrust.

The 12–13 km displacement of the basement above the ramp of the Maestrat Basement Thrust uplifted the 40 km wide area, in the N–S direction, bounded to the N by the Calders monocline, developed above the transition from ramp to flat (Nebot & Guimerà, 2016), during the Late Oligocene – Early Miocene (González, Guimerà & Luzón, 1998).The upper segments of the Mesozoic normal faults across the supra-salt cover were

https://doi.org/10.1017/S001675681600090X Published online by Cambridge University Press

passively transported to the N above the sole thrust flat, experiencing low internal deformation, as this accumulated in the northern external zone, which developed the *N FAT belt* (Fig. 7).

The low angle of the Calders monocline fault-bend fold, and the width of the uplifted area, implies a low dip for the Maestrat Basement Thrust ramp (Nebot & Guimerà, 2016), which was estimated at *c.* 9°, extending southwards for more than 40 km (Fig. 7). The Variscan basement must be involved above this ramp (Nebot & Guimerà, 2016), as it reaches a depth of *c.* 8 km in the upper crust (Fig. 7d). North of it, the acoustic basement fragments incorporated in the thin-skinned thrust system could contain only the Lower Muschelkalk and the Buntsandstein, which vary between 70 and 380 m thick in the exploration wells (Lanaja, 1987), probably having their detachment level at the Buntsandstein top evaporites (Röt facies), as has been deduced in other structures of the Iberian Chain (Ortí, 1981; Guimerà, 1988).

Restoring the Mesozoic supra-salt cover to the end of the Early Cretaceous, the traces at the surface of the normal faults should be displaced southwards a minimum of 12 km (Fig. 7c). The Bordón and Ortells faults become located *c.* 6 km north of the southern antiformal hinge of the Calders monocline, i.e. the Maestrat Basement Thrust transition from ramp to flat (Fig. 7c). In order to link these traces at the surface with the Maestrat Basement Thrust in the acoustic basement, the dip of the normal fault surface across the supra-salt cover should be of *c.* 30°, similar to that obtained in the idealized cross-section for the Ortells fault (Fig. 7a). This indicates that in the area studied, the Maestrat Basement Thrust can be the result of the Cenozoic inversion of the Bordón and the Ortells normal faults (at least its western part), giving additional support to the interpretation of Nebot & Guimerà (2016) that the Maestrat Basement Thrust was the result of the inversion of the Mesozoic normal fault system. The Mesozoic normal faults located N of the Bordón and Ortells faults were cut, during the Cenozoic contraction, by the nearly horizontal short-cut developed within the Middle Muschelkalk detachment, and were transported northwards together with the supra-salt Mesozoic cover. The lower segments of these faults across the acoustic basement should be found in the footwall of the sole thrust, in a more internal position, similarly to the Castellote fault (Fig. 7a).

The orientation and position of the restored normal faults (Fig. 7c) suggest that the present-day arched geometry (salient) of the fold-and-thrust belt (Fig. 2) was partially inherited, as the normal faults during the Mesozoic broadly display an arched geometry (Fig. 7c). During the Cenozoic contraction, this normal fault system was transported northwards within the thrust system, with differential transport, major in the central part, decreasing laterally. In this case, only gentle vertical axis rotation of structures was needed to develop the salient geometry displayed by the fold-and-thrust belt.

7. Conclusions

The Portalrubio–Vandellòs fold-and-thrust belt is the emergence of the Maestrat Basement Thrust, which is the sole thrust of the Cenozoic contractional system. The deep geometry of the latter was deduced after the Calders Monocline, interpreted as a fault-bend fold above a ramp to flat transition. The up-ramp displacement of this basement thrust sheet generated a 40 km wide uplifted area, bounded to the N by the Calders Monocline. Modelling the previous data with the Move® software, a 9° dip for the deep ramp was deduced, extending more than 40 km southwards in the NNE–SSW orientation, and reaching a depth of 7.5 km.

The shortening is estimated to be *c.* 12 km, mostly concentrated at the surface in the northern margin of the thrust belt, being the tectonic displacement towards the NNE. As the sole thrust reached the Mesozoic cover, it propagated through the Middle Muschelkalk evaporitic unit, producing a nearly horizontal detachment, which spread to the N.

Most of the normal faults which bounded the Mesozoic basins were passively transported to the NNE inside the hanging-wall of the Maestrat Basement Thrust, experiencing low internal deformation. Some fragments of the acoustic basement (rocks below the Middle Muschelkalk) were also included.

The palinspastic restoration of the supra-salt cover supports the idea that, in the study area, the Maestrat Basement Thrust is the result of the inversion of the Mesozoic normal fault system in its segment across the basement, and also that the Portalrubio–Vandellòs frontal belt inherited the geometry and orientation of the Mesozoic normal faults.

Acknowledgements. This work was supported by the projects INTECTOSAL (CGL2010-21968-C02-01/BTE) and CGL2008-04916/BTE. The University of Barcelona is acknowledged for a Ph.D. fellowship (APIF) to the first author. The authors also acknowledge Midland Valley and Bentley for providing the Move® and Microstation® software licences. An anonymous reviewer is acknowledged for helpful comments.

References

ALMELA, A., MANSILLA, H., QUINTERO, I. & GÓMEZ, E. 1975. *Oliete, sheet 493. Mapa Geológico de España 1:50.000. 2ª Serie. 1ª Edición*. Madrid: Servicio de Publicaciones, Ministerio de Industria y Energía.

ÁLVARO, M., CAPOTE, R. & VEGAS, R. 1979. Un modelo de evolución geotectónica para la cadena Celtibérica. *Acta Geológica Hispánica* **14**, 172–81.

ANADÓN, P. & ALBERT, J. F. 1973. Hallazgo de una fauna del Muschelkalk en el Trías del anticlinal de Calanda (Provincia de Teruel). *Acta Geológica Hispánica* **8**(5), 151–2.

AURELL, M., MELÉNDEZ, A., SAN ROMÁN, J., GUIMERÀ, J., ROCA, R., SALAS, R., ALONSO, A. & MAS, R. 1992. Tectónica sinsedimentaria distensiva en el límite Triásico-Jurásico en la cordillera ibérica. *Actas del III Congreso Geológico de España* **1**, 50–4.

https://doi.org/10.1017/S001675681600090X Published online by Cambridge University Press

BOVER-ARNAL, T., MORENO-BEDMAR, J. A., FRIJIA, G., PACUAL-CEBRIAN, E. & SALAS, R. 2015. Chronostratigraphy of the Barremian–Early Albian of the Maestrat Basin (E Iberian Peninsula): integrating strontium-isotope stratigraphy and ammonoid biostratigraphy. *Newsletters on Stratigraphy*, **49**(1), 41–68.

CANÉROT, J., CRESPO-ZAMORANO, A. & NAVARRO-VÁZQUEZ, D. 1977. *Montalbán, sheet 518. Mapa Geológico de España 1:50.000. 2ª Serie. 1ª Edición*. Madrid: Servicio de Publicaciones, Ministerio de Industria y Energía.

CANÉROT, J. & LEYVA, F. 1972. *Peñarroya de Tastavins, sheet 520. Mapa Geológico de España 1:50.000. 2ª Serie. 1ª Edición*. Madrid: Servicio de Publicaciones, Ministerio de Industria y Energía.

CANÉROT, J. & PIGNATELLI, R. 1972. *Aguaviva, sheet 519. Mapa Geológico de España 1:50.000. 2ª Serie. 1ª Edición*. Madrid: Servicio de Publicaciones, Ministerio de Industria y Energía.

CANÉROT, J. & PIGNATELLI, R. 1977. *Mosqueruela, sheet 569. Mapa Geológico de España 1:50.000. 2ª Serie. 1ª Edición*. Madrid: Servicio de Publicaciones, Ministerio de Industria y Energía.

ESNAOLA, J. M. & CANÉROT, J. 1972. *Albocácer, sheet 570. Mapa Geológico de España 1:50.000. 2ª Serie. 1ª Edición*. Madrid: Servicio de Publicaciones, Ministerio de Industria y Energía.

GAUTIER, F. 1978. *Alcalà de la Selva, sheet 568. Mapa Geológico de España 1:50.000. 2ª Serie. 1ª Edición*. Madrid: Servicio de Publicaciones, Ministerio de Industria y Energía.

GAUTIER, F. 1979. *Villarluengo, sheet 543. Mapa Geológico de España 1:50.000. 2ª Serie. 1ª Edición*. Madrid: Servicio de Publicaciones, Ministerio de Industria y Energía.

GONZÁLEZ, A. 1989. Análisis tectosedimentario del terciario del borde SE de la Depresión del Ebro (sector bajoaragonés) y de las cubetas ibéricas marginales. Ph.D. thesis, Universidad de Zaragoza, Zaragoza, Spain, 507 pp. Published thesis.

GONZÁLEZ, A., GUIMERÀ, J. & LUZÓN, A. 1998. Edad Oligoceno superior-Mioceno inferior para las superficies de erosión conservadas en el flanco SW de la cubeta de Bordón (Província de Teruel, España). *Geogaceta* **24**, 155–8.

GUIMERÀ, J. 1984. Palaeogene evolution of deformation in the northeastern Iberian Peninsula. *Geological Magazine* **121**(5), 413–20.

GUIMERÀ, J. 1988. Estudi estructural de l'Enllaç entre la Serralada Ibérica i la Serralada Costanera Catalana. Ph.D. thesis, Universitat de Barcelona, Barcelona, Spain. Published thesis. Available at: http://www.tesisenred.net/handle/10803/1936

GUIMERÀ, J. 2004. Cadenas con cobertera: Las Cadenas Ibérica i Costera Catalana. In *Geología de España* (ed. J. A. Vera), pp. 602–7. Madrid: Sociedad Geológica de España & Instituto Geológico y Minero de España.

GUIMERÀ, J. & ÁLVARO, M. 1990. Structure et évolution de la compression alpine dans la Chaîne Ibérique et la Chaîne côtière catalane (Espagne). *Bulletin de la Société Géologique de France* **8**, VI(2), 339–48.

GUIMERÀ, J., GONZÁLEZ, A., SALAS, R. & SANCHO, C. 2010. Origin and preservation of the late contractional relief of an intraplate thrust-belt: the NE Iberian Chain (Iberian Peninsula). *Geophysical Research Abstracts* **12**, EGU2010–5137.

GUIMERÀ, J., MAS, R. & ALONSO, A. 2004. Intraplate deformation in the NW Iberian Chain: Mesozoic extension and Tertiary contractional inversion. *Journal of the Geological Society, London* **161**, 291–303.

LANAJA, J. M. 1987. *Contribución de la exploración petrolífera al conocimiento de la geología de España*. Instituto Tecnológico GeoMinero de España, 465 pp.

MARÍN, PH. & DUVAL, B. 1976. *Castelseras, sheet 495. Mapa Geológico de España 1:50.000. 2ª Serie. 1ª Edición*. Madrid: Servicio de Publicaciones, Ministerio de Industria y Energía.

MARÍN, PH., PALLARD, B., DUVAL, B. & DE MIROSCHEDJI, A. 1974. *Calanda, sheet 494. Mapa Geológico de España 1:50.000. 2ª Serie. 1ª Edición*. Madrid: Servicio de Publicaciones, Ministerio de Industria y Energía.

MARSHAK, S. 2004. Salients, recesses, arcs, oroclines, and syntaxes: a review of ideas concerning the formation of map-view curves in fold-and-thrust belts. In *Thrust Tectonics and Hydrocarbon Systems* (ed. K. R. McClay), pp. 131–56. American Association of Petroleum Geologists, Memoir no. 82.

MARTÍN, L., LEYVA, F. & CANÉROT, J. 1972. *Morella, sheet 545. Mapa Geológico de España 1:50.000. 2ª Serie. 1ª Edición*. Madrid: Servicio de Publicaciones, Ministerio de Industria y Energía.

NAVARRO-VÁZQUEZ, D., CRESPO-ZAMORANO, A., PÉREZ-CASTAÑO, A. & CANÉROT, J. 1972. *Forcall, sheet 544. Mapa Geológico de España 1:50.000. 2ª Serie. 1ª Edición*. Madrid: Servicio de Publicaciones, Ministerio de Industria y Energía.

NEBOT, M. & GUIMERÀ, J. 2016. Structure of an inverted basin from subsurface and field data: the Late Jurassic–Early Cretaceous Maestrat basin (Iberian Chain). *Geologica Acta*, **14**(2), 155–77.

ORTÍ, F. 1981. Diapirismo de materiales triásicos y estructuras de zócalo, en el sector central valenciano (España). *Estudios Geológicos* **37**(3–4), 245–57.

SALAS, R. & GUIMERÀ, J. 1996. Rasgos estructurales principales de la cuenca cretácica inferior del Maestrazgo (Cordillera Ibérica oriental). *Geogaceta* **20**(7), 1704–6.

SALAS, R., GUIMERÀ, J., MAS, R., MARTÍN-CLOSAS, C., MELÉNDEZ, A. & ALONSO, A. 2001. Evolution of the Mesozoic Central Iberian Rift System and its Cainozoic inversion (Iberian chain). In *Peri-Tethys memoir, 6: Peri-Tethyan Rift/Wrench Basins and Passive Margins* (eds P. A. Ziegler, W. Cavazza, A. H. F. Robertson & S. Crasquin-Soleau), pp. 145–86. Mémoires de Muséum National d'Histoire Naturelle, no. 186.

SIMÓN, J. L. 1980. Estructuras de superposición de plegamientos en el borde NE de la cadena Ibérica. *Acta Geológica Hispánica* **15**(5), 137–40.

SIMÓN, J. L. 2004. Superposed buckle folding in the Eastern Iberian Chain, Spain. *Journal of Structural Geology* **26**, 1447–64.